COMPARISON OF THE STRUCTURE OF GRAIN BOUNDARIES IN SILICON AND DIAMOND BY MOLECULAR-DYNAMICS SIMULATIONS*

P. Keblinski[1,2], D. Wolf[1], S. R. Phillpot[1], and H. Gleiter[2]

[1]Materials Science Division
Argonne National Laboratory
Argonne, IL, 60439, USA

[2]Forschungszentrum Karlsruhe
76021 Karlsruhe, Germany

April 1997

Manuscript to be submitted to the Materials Research Society, San Francisco, CA, March 31 - April 4, 1997.

*This work was supported by US Department of Energy BES-Materials Science under Contract No. W-31-109-Eng-38.

COMPARISON OF THE STRUCTURE OF GRAIN BOUNDARIES IN SILICON AND DIAMOND BY MOLECULAR-DYNAMICS SIMULATIONS

P. KEBLINSKI[a,b], S. R. PHILLPOT[a], D. WOLF[a] , H. GLEITER[b]

[a] Materials Science Division, Argonne National Laboratory, Argonne, IL 60439, USA.

[b] Forschungszentrum Karlsruhe, 76021 Karlsruhe, Germany.

ABSTRACT

Molecular-dynamics simulations were used to synthesize nanocrystalline silicon with a grain size of up to 75Å by crystallization of randomly misoriented crystalline seeds from the melt. The structures of the highly-constrained interfaces in the nanocrystal were found to be essentially indistinguishable from those of high-energy bicrystalline grain boundaries (GBs) and similar to the structure of amorphous silicon. Despite disorder, these GBs exhibit predominantly four-coordinated (sp^3-like) atoms and therefore have very few dangling bonds. By contrast, the majority of the atoms in high-energy bicrystalline GBs in diamond are three-coordinated (sp^2-like). Despite the large fraction of three-coordinated GB carbon atoms, they are rather poorly connected amongst themselves, thus likely preventing any type of graphite-like electrical conduction through the GBs.

INTRODUCTION

The electronic and optical properties of polycrystalline silicon films are significantly affected by the presence of grain boundaries (GBs).[1] For example, GBs can provide active sites for the recombination of electron-hole pairs, important in photovoltaic application. Because of silicon's strong energetic preference for sp^3-hybridization over other electronic configurations, the structural disorder in silicon GBs is accommodated by a distortion of the tetrahedral nearest-neighbor bonds and, in the extreme, by the creation of dangling bonds.

By contrast, carbon can form both sp^3- and sp^2-hybridized electronic states, as evidenced by the existence of two energetically rather similar bulk phases, diamond and graphite, and by the spectrum of amorphous forms of carbon ranging from low-density sp^2-like structures to the denser diamond-like amorphous carbon. Also, the typically three to five times higher elastic moduli of diamond by comparison with those of Si indicate nearest-neighbor bonds that are much stiffer with respect to both bond bending and bond stretching. Intuitively one would expect that both effects would result in less structural disorder in diamond GBs: diamond-like carbon atoms in structurally disordered environments should be able to accommodate a relatively lesser amount of bond distortion before changing hybridization from sp^3 to sp^2, thus remaining structurally more ordered while enabling bond-coordination disorder.

In this paper we analyze in some detail the structure of GBs in a model Si nanocrystal generated by molecular-dynamics (MD) simulations and find that they are amorphous. Moreover, by simulating representative high-energy GBs in Si bicrystals we demonstrate that such intergranular amorphous structures are thermodynamically stable. We compare the calculated structures of one representative GB in Si and diamond, and show that, in sharp contrast to Si, the diamond GB is structurally ordered but has a large number of sp^2-bonded atoms. We discuss the implications of this result for nanocrystalline diamond.

NANOCRYSTALLINE SILICON

Molecular-dynamics simulations and the Stillinger-Weber empirical potential for silicon [2] were used to synthesize nanocrystalline microstructures by crystallization of randomly misoriented crystalline seeds from the melt. The three-dimensionally (3d) periodic cubic simulation cell used in our simulations is sketched in Fig. 1. The starting configuration consists of an fcc arrangement of four randomly oriented seed grains of diamond structured Si embedded in the melt filling the rest of the cell. The random orientations of the seeds usually result in GBs having both

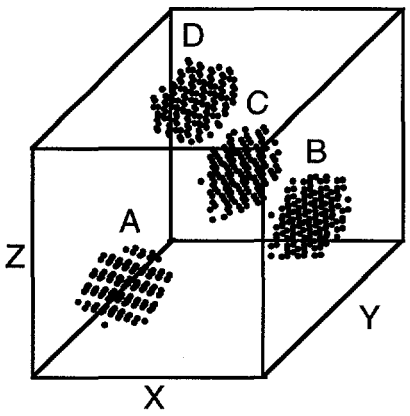

Fig. 1. Cubic, 3d periodic simulation cell containing four randomly oriented seed grains arranged on an fcc lattice and embedded in the melt.

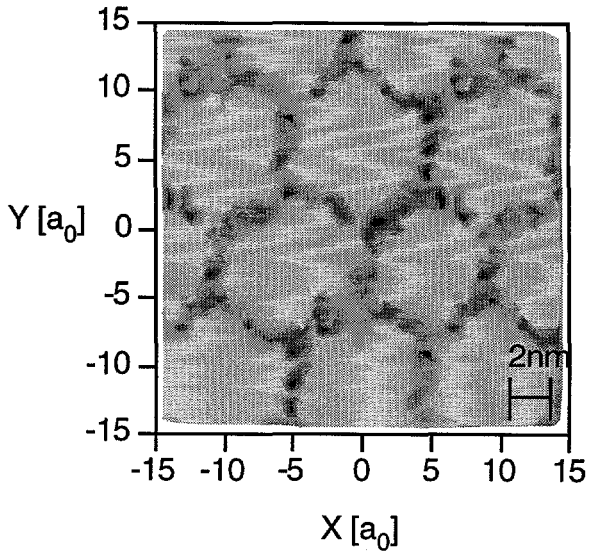

Fig. 2. Energy-per-atom gray-scale contour plot for a (111) slice through the fcc microstructure that contains the centers of all four grains. Dark regions indicate high excess energy while the light grain interiors are perfectly crystalline.

tilt and twist components; i.e., "general" boundaries (by contrast with symmetric or with "special" GBs). The simulation procedure, described in details in Ref. 3, consisted of melting the system at high-temperature while the seed atoms were kept fixed at their perfect-crystal positions, gradually rotating the seeds to randomly chosen orientations and then cooling down to T=1250 K, (i.e., well below the melting point, T_m =1690K) thereby generating a thermodynamic driving force for crystal growth, proportional to T_m-T. During this growth a constant-pressure algorithm was applied to relax the system to zero external pressure and the system was allowed to evolve freely with no constraints imposed on the seed atoms. The growth continued until the internal energy of the system stopped decreasing. Finally the system was cooled down by rescaling the velocities of the atoms to T=0 K under zero external pressure.

To characterize the fcc microstructure thus obtained, we make planar cuts of thickness $0.5a_0$ through the simulation cell (a_0=5.43Å is the zero-temperature lattice parameter). Figure 2 shows gray-scale contours of equal energy per atom for a slice parallel to the microstructural (111) planes for the system with the grain size d=5.4 nm; this cut slices through all four grain centers (see also Fig. 1). Clearly, all GBs (seen as dark lines) have roughly the same width while the triple lines (where the GB meet) appear to be slightly wider than the GBs. These structural features are independent of the grain size for the three grain size simulated d=3.8, d=5.4 and d=7.8 nm.[3]

The atomic structure in the inhomogeneous regions of the material may be characterized by *local* radial distribution functions, such as those shown in Fig. 3 associated with atoms in the GBs, triple lines, and point junctions. Strikingly, all these local distributions are remarkably similar to the overall G(r) of bulk amorphous silicon also shown in Fig. 3, indicating a virtually complete absence of long-range order in these locally disordered environments. Thus our model microstructure with randomly-misoriented grains can be viewed as a two-component system; crystalline grain interiors connected by a glue-like disordered phase similar to that of amorphous silicon.

THERMODYNAMIC STABILITY OF THE AMORPHOUS INTERGRANULAR FILM

To elucidate the origin of the amorphous intergranular phase present in our model nanocrystalline microstructures, we have investigated the atomic structures of bicrystalline Si GBs. [4] Because (i) the GBs in our model nanocrystalline materials have relatively high energies and

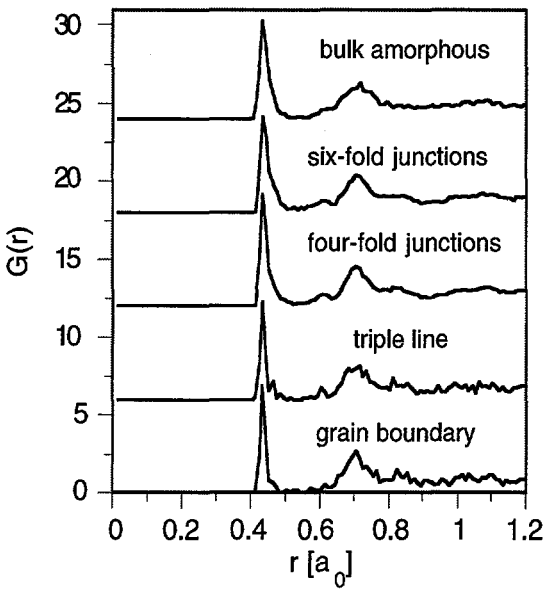

Fig. 3. *Local* radial distribution functions in the GBs and grain junctions for the microstructure with the intermediate grain size (~5.4 nm). For comparison, G(r) for bulk amorphous silicon is also shown.

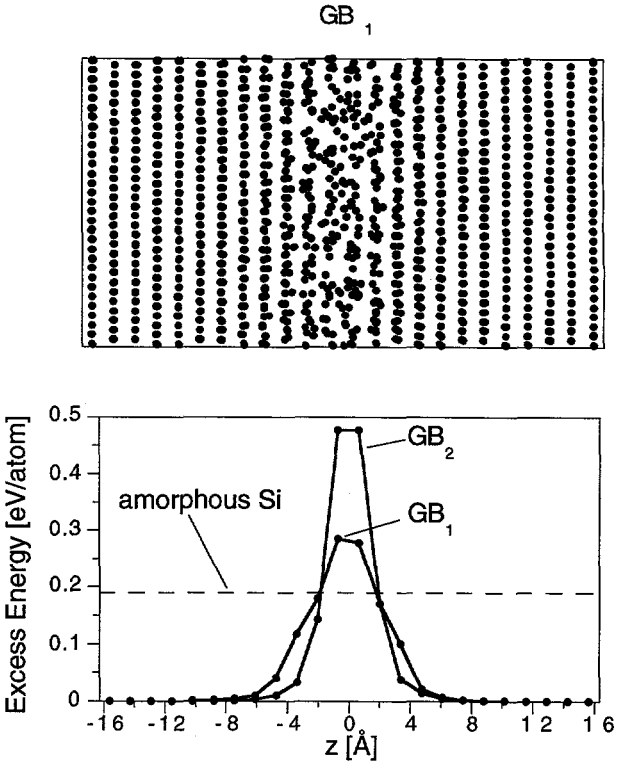

Fig. 4. Projected positions of the atoms for the (100) $\phi = 43.60^\circ$ (Σ 29) twist GB in Si. Upper panel: high-temperature relaxed structure (GB_1). Lower panel: average energy per atom in (100) slices of thickness $0.25a_0$ as a function of distance, z, from the GB. The dashed line shows the cohesive energy of bulk amorphous Si for the SW potential.

(ii) low-energy ("special") Si GBs are well known to be crystallographically ordered [5], we have studied high-angle symmetric *twist* boundaries which are known to have generally higher energies than symmetric *tilt* boundaries [6]; they therefore appear more likely to disorder while lowering their energy upon high-temperature equilibration than do tilt boundaries

To test the independence of the GB structure on the details of the high-temperature treatment, the bicrystal was subjected to two distinct high-temperature treatments. Starting from the zero-temperature relaxed structure, in the first treatment a large number of planes around the GB were melted and subsequently regrown (analogous to the method used above for synthesizing the nanocrystalline microstructures). In the second treatment the zero-temperature relaxed GB was simply annealed at T=1500 K (190 K below T_m) and then cooled back down to zero temperature. In all cases the two treatments yielded GB structures with practically the same overall characteristics (radial and bond-angle distribution functions and energy profiles), although the detailed atomic structures and GB energies were not completely identical. We first present in some detail results for the (100) $\phi = 43{\cdot}60^\circ$ (Σ29) twist GB. Its high-temperature equilibrated (GB_1) structure is shown in the top panel in Fig. 4. The related plane-by-plane profiles of the average-per-atom excess energy over the perfect-crystal cohesive energy is shown in the bottom panel. While the GB_2 profile is rather narrow with a maximum value of 0.47 eV, the GB_1 profile is broader but its peak value is only 0.27 eV. Despite the GB_1 energy profile being broader, the related GB energy (the integral under the energy profile) of 1340 erg/cm^2, is approximately 10% lower than the energy of GB_2 (1464 erg/cm^2 [7]). The lowering of the energy during high-temperature equilibration, demonstrates a thermodynamic origin for this restructuring.

The loss of crystalline order in the center of GB_1 is evident from the related *local* radial and bond-angle distribution functions [4] which are strikingly similar to those of bulk amorphous Si (see also Fig. 4). Furthermore, consistent with results for bulk amorphous Si using the same potential [8], in the disordered region of GB_1 only about 1.5% of the atoms are 3-fold coordinated (i.e., atoms with dangling bonds) while 83.5% are 4-fold and 15% are 5-fold coordinated. By comparison, GB_2 structure is considerably less-well coordinated, with 6% of the atoms having dangling bonds. [4]

The origin of the driving force for the GB disordering process is apparent from the bottom panel of Fig. 4. The peak energy of 0.47 eV/atom for the GB_2 structure far exceeds the average excess energy per atom in bulk amorphous Si of 0.185 eV (dashed line). By contrast, in the most disordered plane of GB_1 the average excess energy is only 0.27 eV/atom, much closer to the excess energy of amorphous Si. That the energy in the GB region does not reach that of the amorphous phase is a manifestation of the confinement arising from the presence of nearby crystalline regions.[4]

Based on these insights, one might expect that all high-energy GBs should have similar, "confined-amorphous" structures. To test this prediction we investigated three other high-angle, high-energy twist boundaries with qualitatively different zero-temperature relaxed structures: (100) $\phi = 61.93^\circ$ (Σ 17), (110) $\phi = 44.00^\circ$ (Σ 57) and (112) $\phi = 35.26^\circ$ (Σ 35). We found that high-temperature relaxation lowers the energies of all these GBs to values in the range of 1300-1370 erg/cm^2. Moreover, despite being sandwiched between different crystallographic surfaces, all the GBs were found to be disordered and structurally very similar to each other [4], to those obtained for the GBs in nanocrystalline Si [3] and to bulk amorphous Si [8].

By contrast with these disordered structures for high-energy GBs, one might expect that low-energy GBs should not disorder upon high-temperature equilibration. To confirm this prediction we studied the (111), ϕ=42.10° (Σ 31) twist GB, also a *high-angle* GB, however on the most widely-spaced and hence, lowest-energy plane in the diamond structure, with a zero-temperature relaxed energy of only 638 erg/cm^2 [7]. Indeed, as expected, neither its structure nor its energy change during high-temperature annealing and the GB remains crystalline right up to the GB plane.

COMPARISON OF SILICON AND DIAMOND GBs.

We will focus our comparison of diamond and Si interfaces on the (100) $\phi = 43{\cdot}60^\circ$ (Σ29) high-energy GB which, as described above, is representative the GBs present in nanocrystalline microstructure with more or less randomly misoriented grains. Also geometrically, (100) twist GBs are representative of a typical random plane in diamond crystal since they involve GB atoms having 50% (two out of four) bonds across the interface (remaing bonds are with atoms on the same side of GB). To enable a clear comparison, we used Tersoff's potential for diamond [9] and silicon [10]. As in our previous studies the zero-temperature relaxed structures were annealed at about 80% of the melting point, and subsequently cooled to the zero temperature.

The results for the Si grain boundary using the Tersoff potential were qualitatively the same as those discussed above for the SW potential. In particular, with the Tersoff potential high-temperature relaxation disorders the GB and lowers its energy by over 20%. This energy lowering is accompanied by a reduction in the number of dangling bonds from 50% to 8%; the structure of the most disordered planes in this GB are similar to the bulk amorphous phase.

By contrast, in the diamond GB high-temperature equilibration shows little effect on coordination or energy. Even after annealing, the diamond GB shows good crystalline order. Most notably, however, about 80% of the atoms in the two atomic planes at the GB are 3-coordinated. This behavior suggests that sp^2-bonded C atoms, already present in the zero-temperature relaxed structure, experience virtually no driving force for becoming sp^3-bonded. By contrast, because sp^2-hybridization is not a choice for Si, a huge driving force exist for the Si atoms to become four-fold coordinated, however at the prize of the structural disordering.

These differences between the structures of the diamond and silicon GBs are depicted in Fig. 5, showing atomic positions and bonding between atoms at or near the GB for the two structures. The Si GB is characterized by a disordered, amorphous structure, whereas the diamond GB is more ordered, however with far fewer inter-atomic bonds across the GB.

The different nature of bonding in these diamond and silicon GBs is also illustrated by the bond-angle distribution functions showed in Fig. 6. Both distributions are relatively broad, and

Diamond

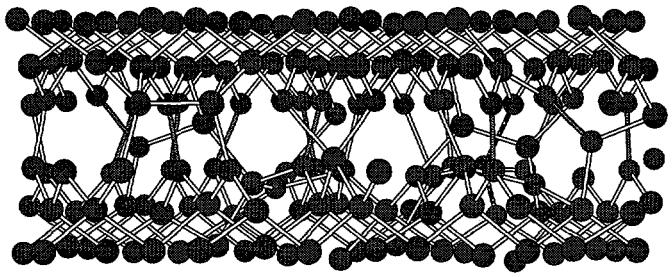

Silicon

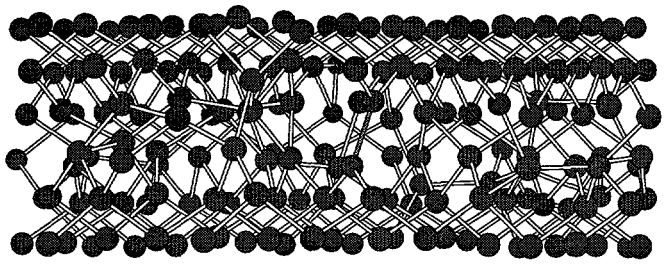

Fig. 5. Projected bonding structures of the high-temperature relaxed (100) (S29) twist boundary in diamond and Si. Rather strikingly, with 80% of the GB atoms being three coordinated, the diamond boundary exhibits a lot fewer bonds across the GB than the Si boundary, in which 82% of the atoms are four coordinated.

similar to those obtained for bulk-amorphous material. However, whereas in the diamond GB the distribution is peaked near the graphite (sp^2-hybridized) bond angle of 120°, in Si the distribution is peaked near the tetrahedral (sp^3-hybridized) bond angle of 109°.

The differences in the structures of diamond and silicon GBs are readily understood in terms of the preferential sp^2-bonding at the diamond GB. When initially forming the GB by bringing two misoriented free (100) surfaces into contact, two of the four bonds of every C atom at the GB involve atoms across the GB. However, in the fully relaxed diamond GB 80% of the atoms are three coordinated meaning approximately 40% of all bonds across the interface were lost due to the change in hybridization from sp^3 to sp^2. Hence, in spite of the fact that in the perfect crystalline graphite sp^2 bonds are about 5% shorter than sp^3 bonds the GB expands significantly while stretching many of the initially tetrahedrally oriented bonds so as to point rather directly across the GB. By contrast, in the Si GB most of the atoms retain their usual four nearest neighbors even at the price of becoming structurally disordered; the result is a highly dense, albeit disordered GB.

Finally, we investigate the degree of connectivity amongst the three-coordinated carbon atoms in the GB. Despite the fact that 80% of the atoms in the two GB planes are three coordinated, other than for the sp^2 bonded atom pairs connected across the GB there is very little in-plane connectivity. It appears that the reason for this low connectivity is mostly geometrical. Three coordinated atoms are not bonded within the (100) planes, typically two of the three bonds of each GB atom involve four-coordinated atoms within the same grain while only one bond is capable of connecting with another three-coordinated atom, however across the GB. Given the geometrical origin of this behavior and the fact that the (100) planes are geometrically representative of all high-energy GB planes, it appears that this behavior is generic to high-angle high-energy twist GBs in diamond.

CONCLUSIONS

One motivation for comparing Si and diamond GBs was that the atomic structures and energies of Si boundaries provide a basis for understanding GB structural disorder in a purely sp^3-bonded material against which the greater bond stiffness in diamond combined with its ability to change hybridization in a defected environment from sp^3 to sp^2 can be elucidated. In silicon, a purely sp^3-bonded material, in a defected environment a large driving force exists to maintain the four-fold nearest-neighbor coordination as much as possible, even at the price of bond-bending and bond-stretching so as to completely disorder the GB. By contrast in diamond, as a consequence of its greater bond stiffness and its ability to change hybridization, bond disorder is energetically much more costly; already relatively small bond distortions are therefore capable of locally inducing sp^2-type bonding. This competition between disordering and local coordination translates into considerably more ordered GB structures than in Si, which are sp^2-hybridized.

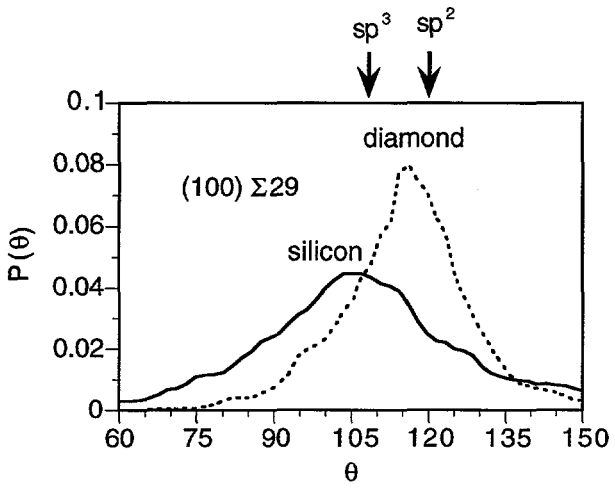

Fig. 6. Bond-angle distribution function, P(θ) (in arbitrary units), for atoms in the two center planes of the (100) Σ29 GB in silicon and diamond.

Studies of nanocrystalline and extended GBs in silicon suggest that microstructures with more or less randomly oriented grains are characterized by predominantly high-energy, general GBs. Thus, without actually simulating nanocrystalline diamond, we can gain insights into the nature of its interfaces from our studies of a high-angle, high-energy twist GB on (100) which is geometrically representative of virtually all high-energy GB planes in diamond crystal structure.

We found that despite losing about 40% of the bonds across the GB, the high-energy GBs in diamond are very stable and are characterized by large a work of adhesion. This stability is directly due to the relatively large number of sp^2-bonds connecting the grains and may well be the main reason for the overall structural and mechanical stability of nanocrystalline diamond. [11,12]

Finally we speculate on the electrical behavior of the nanocrystalline diamond. Despite ~80% of the atoms in a typical diamond GB being three-coordinated, the graphite like electrical conductivity through interfaces in the nanocrystalline diamond is not likely, due to the poor connectivity of the three-coordinated atoms. Whether surface or GB reconstruction, possibly under the effect of bridging hydrogen, can induce such behavior remains an open question.

ACKNOWLEDGMENTS.

PK gratefully acknowledges support from the A. v. Humboldt Foundation. SRP and DW are supported by the US Department of Energy, BES-Materials Science under Contract No. W-31-109-Eng-38.

REFERENCES

1. See, for example, papers in *Polycrystalline Semiconductors*, edited by H.-J. Möller, H. P. Strunk and J. H. Werner, Springer Proceedings in Physics Vol. 35 (Springer, Berlin, 1989); *Polycrystalline Semiconductors II,* edited by J. H. Werner and H. P. Strunk, Springer Proceedings in Physics Vol. 54 (Springer, Berlin, 1991).
2. F. H. Stillinger and T. A. Weber, Phys. Rev. B **31**, 5262 (1985).
3. P. Keblinski, S. R. Phillpot, D. Wolf and H. Gleiter, Acta. Mat. **45**, 987 (1997); Phys. Lett. A **226**, 205 (1997).
4. P. Keblinski, S. R. Phillpot, D. Wolf and H. Gleiter, Phys. Rev. Lett. **77**, 2965 (1996); J. Amer. Ceram. Soc. **80** 717 (1997).
5. A. Bourret and J. J. Bacmann, Surface Science **162**, 495 (1985).
6. See, for example, D. Wolf and K. L. Merkle in *Materials Interfaces: Atomic-Level Structure and Properties*, edited by D. Wolf and S. Yip (Chapman and Hall, 1992), p. 87 ff.
7. S. R. Phillpot and D. Wolf, Phil. Mag. A **60**, 545 (1989).
8. W. D. Luedtke and U. Landman, Phys. Rev. B **37,** 4656 (1988); ibid. **40,** 1164 (1989).
9. J. Tersoff, Phys. Rev. B **38**, 9902 (1988).
10. J. Tersoff, Phys. Rev. Lett. **61**, 2879 (1988).
11. N. M. Hwang, J. H. Hahn and D. Y. Yoon, J. Cryst. Growth **160**, 87 (1996); N. M. Hwang and D. Y. Yoon, ibid. **160**, 98 (1996).
12. R. Csencsits, C. D. Zuiker, D. M. Gruen and A. R. Krauss, Solid State Phen. **51-52**, 261 (1996).